Collective dynamics in a liquid polyvalent metal: Liquid thallium at the melting point

Taras Bryk[1,a] and J.-F. Wax[2]
[1]*Institute for Condensed Matter Physics, National Academy of Sciences of Ukraine, 1 Svientsitskii Street, UA-79011 Lviv, Ukraine and Institute of Applied Mathematics and Fundamental Sciences, National Polytechnic University of Lviv, UA-79013 Lviv, Ukraine*
[2]*Laboratoire de Physique des Milieux Denses, Université Paul Verlaine Metz, 1, Boulevard Arago 57078 Metz Cedex 3, France*

(Received 25 September 2009; accepted 24 January 2010; published online 18 February 2010)

Collective dynamics in liquid thallium at the melting point in a wide range of wave numbers and frequencies is studied by molecular dynamics simulations and a theoretical analysis of time correlation functions within the approach of generalized collective modes. The heat fluctuations were explicitly treated in the theoretical scheme within the thermoviscoelastic dynamic model. We report dispersion and damping of generalized longitudinal sound excitations, nonhydrodynamic shear and heat waves, as well as wave number dependence of main relaxation processes. Generalized wave number-dependent thermodynamic quantities and transport coefficients in liquid Tl are discussed. © *2010 American Institute of Physics*. [doi:10.1063/1.3319500]

I. INTRODUCTION

Collective dynamics in liquids is among the most fascinating fields of condensed matter physics. Microscopic dynamics even in pure fluids is much less understood on a molecular-size scale than phonon dynamics in crystals or vibrational dynamics of glasses.[1] Among all the fluids, liquid metals are of special interest because they display well-defined collective excitations over a wide range of wave numbers, k, as observed in inelastic neutron scattering and inelastic x-ray scattering experiments.[2] The hydrodynamic theory, which is valid on macroscopic space and time scales, predicts via the Landau–Placzek ratio[3] that the pronounced side peaks of the dynamic structure factors $S(k,\omega)$ can be observed in liquids whose ratio of specific heats $\gamma=C_P/C_V$ is close to unity. In liquid metals γ usually ranges from $\sim$1.06 for liquid lithium up to $\sim$1.8–1.98 for liquid transition metals such as Fe, Co, and Ni.[2]

The shape of time correlation functions as well as the main contributions to them can only be predicted analytically on macroscopic time and space scales, where the local conservation laws correspond to the hydrodynamic equations.[4] Time correlation functions between collective dynamic variables are the main quantities for a theoretical treatment of liquid dynamics. On a length scale, when the atomic structure of the liquid becomes distinguishable, all the dynamic processes show a crossover from a hydrodynamic behavior to an atomic one. There does not exist a single theory, which correctly describes all the variety of microscopic collective processes existing on the atomic scale and coupling effects between them. A significant breakthrough in understanding the liquid dynamics on different length scales was achieved when molecular dynamics (MD) computer simulations made available calculations of density-density time correlation functions $F_{nn}(k,t)$ and their time Fourier transforms known as dynamic structure factors $S(k,\omega)$, where k and ω are the wave number and frequency, respectively. However, the MD-derived time correlation functions are of little use in themselves because the information on the different collective processes is hidden in their shape and one does not *a priori* know what kind of collective processes contribute to the $F_{nn}(k,t)$ (except in the case of extremely small wave numbers, where the main contributions are known from hydrodynamic theory). It is generally agreed that the leading oscillating contribution to the shape of $F_{nn}(k,t)$ comes from the acoustic excitations, while one cannot separate and estimate the strength and origin of the different relaxation processes contributing to these time correlation functions beyond the hydrodynamic regime. Besides, the widely used purely numerical procedure of estimating the dispersion of collective excitations from the positions of the side peak of $S(k,\omega)$ is only valid in a rather narrow long-wavelength range, where the overlap between the central and side peaks is negligible. Another numerical approach for this evaluation is based on the positions of the peak of the spectral function of the longitudinal current,

$$C^L(k,\omega)=\frac{\omega^2}{k^2}S(k,\omega),$$

and yields frequencies slightly shifted with respect to those obtained from the positions of the side peaks of $S(k,\omega)$, as follows from the above relation. It is obvious that a consistent definition of collective excitations in liquids must have a correct analytical basis and lead to identical dispersion of acoustic excitations when obtained either from $S(k,\omega)$ or from $C^L(k,\omega)$.

In order to accurately and consistently estimate the dispersion of the collective excitations as well as the origin of

[a]Electronic mail: bryk@icmp.lviv.ua.

the main collective processes responsible for the shape of time correlation functions in different ranges of wave numbers, one has to perform their analysis based on correct models of generalized hydrodynamics. Many computational studies restrict the analysis by simply using fitting procedures based on the oversimplified damped harmonic oscillator model. In other studies one applies the hydrodynamic expressions for analysis of $F_{nn}(k,t)$, which obviously are incorrect beyond the hydrodynamic regime. The hydrodynamic regime itself is difficult to reach in MD simulations, even at the smallest wave numbers accessible. For this purpose, very large simulation systems are required, typically of more than 2000 particles.

In order to be efficient at describing the collective dynamics of liquids over a wide range of wave numbers, generalized hydrodynamic models must account for the existence of nonhydrodynamic collective processes such as structural relaxations, etc. Furthermore, these dynamic models must correctly reproduce the long-wavelength asymptotes of the main hydrodynamic processes: acoustic modes and nonpropagating relaxation processes connected with thermal diffusivity and shear viscosity. Another important point in analyzing the collective dynamics of liquids is the need of an explicit treatment of heat fluctuations in the system. Analysis of heat fluctuations from MD simulations of liquids is very rare in the literature, even within the widely used memory function formalism.[5] The most complete scheme proposed so far to take into account thermal fluctuations within the generalized hydrodynamic theory is a generalized collective modes (GCM) approach.[6] It is based on the treatment of a hierarchy of dynamic variables, which is extended from the hydrodynamic ones in order to take into account effects existing on shorter time scales than hydrodynamic processes. Such a generation of extended dynamic variables is applied to all the hydrodynamic variables (such as particle density, heat density, concentration densities in many-component case, etc.) in order to reach the desired level of accuracy in the description of short-time processes in liquids. All the N_v hydrodynamic and extended dynamic variables form the so-called basis set of dynamic variables, which is used to estimate the generalized hydrodynamic matrix, $\mathbf{T}(k)$. Within the GCM approach, the collective excitations are defined as the eigenvalues of the generalized hydrodynamic matrix, $\mathbf{T}(k)$, being thus in complete agreement with the generally adopted definition of collective excitations in statistical physics as poles of the relevant Green functions. Hence, the N_v eigenvalues $z_\alpha(k)(\alpha=1,\ldots,N_v)$ of the $N_v \times N_v$ generalized hydrodynamic matrix represent microscopic collective processes in the liquid on length scales corresponding to the wave number value k.

The GCM approach proved to be accurate in describing the hydrodynamic and nonhydrodynamic modes of simple metal Cs,[7] polyvalent liquid metals Bi and Pb,[8] as well as liquid metallic alloys Mg–Zn and Li–Pb.[9] To date, the GCM approach is perhaps the most correct *parameter-free method* for analyzing time correlation functions and evaluating nonhydrodynamic processes in liquids. It is supported by numerous analytical results for nonhydrodynamic relaxation and propagating processes.

In this study we aimed to apply the well-tested GCM approach to the exploration of collective dynamics in a trivalent liquid metal, namely, Tl, at its melting point. There were no GCM studies of collective excitations and relaxation processes in trivalent liquid metals before. Therefore, we aimed to obtain the spectrum of propagating and relaxation eigenmodes for liquid Tl over a wide range of wave numbers, in order to trace back to their origin and estimate their long-wavelength asymptotes from which different thermodynamic quantities and transport coefficients can be calculated. The paper is organized as follows. In Sec. II, we shortly describe the details of our MD simulations and GCM analysis. Section III contains the analysis of the dynamic eigenmodes in liquid Tl obtained within a five-variables thermoviscoelastic model, while Sec. IV summarizes the conclusions of this study.

II. DETAILS OF MD SIMULATIONS

We performed MD simulations for a system of 4000 particles with number density matching the experimental value $n=0.033$ Å^{-3} (Ref. 10) under periodic boundary conditions in NVT ensemble. The reliability of the model of interactions is a crucial point when performing simulations of real systems. Indeed, it is necessary to reproduce with the highest accuracy the forces between the atoms in order for the simulated system to behave as similarly to the real one as possible. Therefore, the quality of the interaction model needs to be tested versus experiments. Trivalent metals are not as easy to describe as alkali ones and efficient potential models are rather scarce. In this study, the effective two-body interaction potential for liquid metallic Tl was obtained using Fiolhais local pseudopotential to describe the electron-ion interaction and Ichimaru–Utsumi local-field correction function to account for exchange and correlation effects. This two-body effective potential was tested previously by computing the static structure factor $S(k)$ and evaluating the melting temperature of Tl.[11] Obtained $S(k)$ was in very nice agreement with the experimental one at the melting temperature,[12] which was estimated at 590 ± 20 K,[11] in quite good agreement with the experimental value of 577 K.

The time step was 10 fs in our simulations. The production run was 300 000 steps long and each sixth configuration was used to evaluate the static averages and time correlation functions. The high accuracy of the elements of the generalized hydrodynamic matrix thus reached is required by the GCM approach in order to avoid any unphysical behavior of the dynamic eigenvalues.

Twenty k-points were considered when estimating the k-dependent quantities. The smallest k-value reached in the current study was 0.127 Å^{-1}. Averages over all the wave numbers with identical absolute value but different directions were performed. For each k-point the elements of the generalized hydrodynamic matrix $\mathbf{T}(k)$ were directly estimated from MD simulations avoiding any fitting procedure. The GCM analysis of time correlation functions for liquid Tl was performed within a thermoviscoelastic five-variables dynamic model,

$$\mathbf{A}^{(5)}(k,t) = \{n(k,t), J^L(k,t), \varepsilon(k,t), \dot{J}^L(k,t), \dot{\varepsilon}(k,t)\}, \quad (1)$$

for the case of longitudinal dynamics and a two-variables dynamic model,

$$\mathbf{A}^{(2T)}(k,t) = \{J^L(k,t), \dot{J}^T(k,t)\}, \quad (2)$$

for transverse case. The dynamic variables for density $n(k,t)$, density of longitudinal/transverse mass-current $J^{L/T}(k,t)$, and energy density $\varepsilon(k,t)$ are the hydrodynamic ones and are represented as follows:

$$n(k,t) = \frac{1}{\sqrt{N}} \sum_{j=1}^{N} e^{-i\mathbf{k}\mathbf{r}_j},$$

$$J^L(k,t) = \frac{m}{\sqrt{N}} \sum_{j=1}^{N} \frac{\mathbf{k}\mathbf{v}_j}{k} e^{-i\mathbf{k}\mathbf{r}_j}, \quad (3)$$

$$J^T(k,t) = \frac{m}{\sqrt{N}} \sum_{j=1}^{N} \frac{[\mathbf{k}\mathbf{v}_j]}{k} e^{-i\mathbf{k}\mathbf{r}_j},$$

$$\varepsilon(k,t) = \frac{1}{\sqrt{N}} \sum_{j=1}^{N} \varepsilon_j e^{-i\mathbf{k}\mathbf{r}_j},$$

where N and m are the number and mass of particles in simulations, and ε_j is the single-particle energy of the jth particle, which can easily be calculated in the case of effective pair potentials such as used in our MD simulations. The square brackets in expression for transverse mass-current mean the vector product. The dotted variables in Eqs. (1) and (2) are the extended ones and represent the first time derivatives of the corresponding hydrodynamic variables (3). Their explicit expressions follow directly. All the five longitudinal and two transverse dynamic variables were easily sampled straight from MD simulations. The time evolution of these dynamic variables was used to estimate the matrix of time correlation functions, $\mathbf{F}(k,t)$, and the corresponding elements of the generalized hydrodynamic matrix,

$$\mathbf{T}(k) = \tilde{\mathbf{F}}(k, z=0)\mathbf{F}^{-1}(k, t=0),$$

where $\tilde{\mathbf{F}}(k,z=0)$ is the matrix of Laplace-transformed correlation functions in Markovian approximation. The generalized hydrodynamic matrix was calculated for each k-point sampled in MD and corresponding eigenvalues were estimated. We recall that as many eigenvalues as the considered dynamic variables are to be determined. As we will see, they can either be pairs of complex conjugated eigenvalues (propagating modes) or purely real ones (relaxation modes). Moreover, it may happen at given k-values that two real eigenvalues merge into a pair of complex ones, or vice versa. In the range of small wave numbers the resulting eigenmodes can be compared with the analytical five-mode solution of the dynamic model $\mathbf{A}^{(5)}(k,t)$ in the long-wavelength limit.[13]

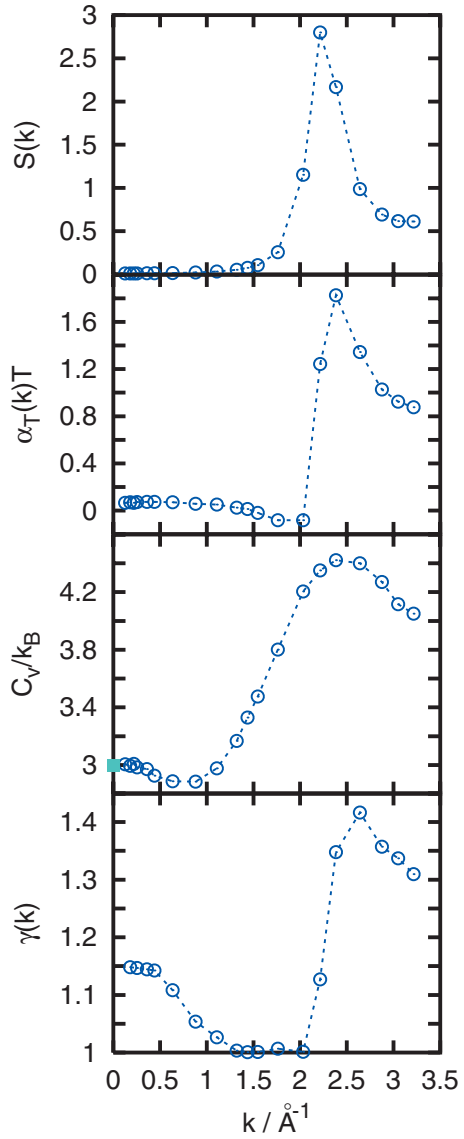

FIG. 1. Structure factor $S(k)$ for liquid Tl at the melting point and wave number-dependent thermodynamic quantities: generalized linear thermal expansion coefficient $\alpha_T(k)$, generalized specific heat at constant volume $C_V(k)$, and generalized ratio of specific heats $\gamma(k)$. The experimental value of γ, namely, 1.14 (Ref. 2), can be recovered by extrapolation of $\gamma(k)$ to the limit $k \to 0$.

III. RESULTS AND DISCUSSION

A. Static properties

Static structure factor $S(k)$ can be calculated from the MD data using either pair distribution function $g(r)$ or statistical averages of instantaneous density-density correlations. Having the main dynamic variables (3) sampled in MD simulations it is straightforward to estimate via statistical averages all the wave number-dependent thermodynamic quantities using the known expressions.[14,15] The static structure factor $S(k) = \langle n(-k)n(k) \rangle$ of liquid Tl at the melting point is shown in the top frame of Fig. 1. It perfectly reproduces the previous results.[11] We will keep in mind that the main peak of the $S(k)$ is located at ~ 2.2 Å^{-1}. Calculations of other generalized wave number-dependent thermodynamic

quantities permit to verify whether the effective pair potentials used in this study enable one to simulate correctly the heat density fluctuations in the liquid polyvalent metal.

The wave number dependences of generalized linear thermal expansion coefficient $\alpha_T(k)$, generalized specific heat at constant volume $C_V(k)$, and generalized ratio of specific heats $\gamma(k)$ are shown in Fig. 1. They display their maxima close to the location of the main peak of static structure factor. It is interesting to notice that the generalized linear thermal expansion coefficient takes negative values in the region 2.1 $\text{Å}^{-1} > k > 1.6$ Å^{-1}. Similar behavior of $\alpha_T(k)$ was observed in the case of liquid Pb close to the melting point.[8] The generalized specific heat at constant volume $C_V(k)$ has a minimum at ~ 0.75 Å^{-1}, while with further decrease in wave number the $C_V(k)$ smoothly increases right to the macroscopic value $C_V = 2.98$ k_B, which was obtained directly from the temperature fluctuations during the MD run. Another generalized thermodynamic quantity, the generalized ratio of specific heats $\gamma(k)$, reflects the strengths of coupling between thermal and viscous processes. For $\gamma = 1$ the coupling between the two types of processes vanishes. One can see that in the region 2.0 $\text{Å}^{-1} > k > 1.3$ Å^{-1} the cross correlation between thermal and viscous processes is almost absent, while it is very important at the location of the main peak of static structure factor. The wave number dependence $\gamma(k)$ smoothly reaches a macroscopic value when $k \to 0$, which is in perfect agreement with the experimental value of 1.14.[2]

B. Time correlation functions and dynamic structure factors

Time correlation functions between hydrodynamic variables contain in their shape information about all the microscopic collective processes and coupling effects between them. Successful theoretical approaches to collective dynamics of liquids have to reproduce the MD-derived time correlation functions. The main advantage of the GCM approach over the regular memory function method is the simultaneous fulfillment of sum rules for three hydrodynamic time correlation functions: density-density, density-energy, and energy-energy time correlation functions. Within the dynamic model $\mathbf{A}^{(5)}(k,t)$, the density-density time correlation function fulfills the sum rules up to the fourth frequency moment of the dynamic structure factor, while the density-energy and energy-energy functions reach up to the third and second frequency moments of the corresponding spectral functions, respectively.

The GCM approach requires the knowledge of wave number-dependent correlation times $\tau_{ij}(k)$, which can be calculated directly from the MD-derived time correlation functions. The requirement of equivalence between $\tau_{ij}(k)$ obtained from the MD-derived functions and their GCM replicas forms additional sum rules for zero time moments of corresponding time correlation functions.

In Fig. 2 one can see the quality of GCM replicas of density-density, density-energy, and energy-energy time correlation functions. The frequency and decay rate of the oscillations of the MD-derived functions are perfectly reproduced by the GCM replicas, so that one can expect the dynamic model $\mathbf{A}^{(5)}(k,t)$ to be able to correctly take into account the main microscopic processes.

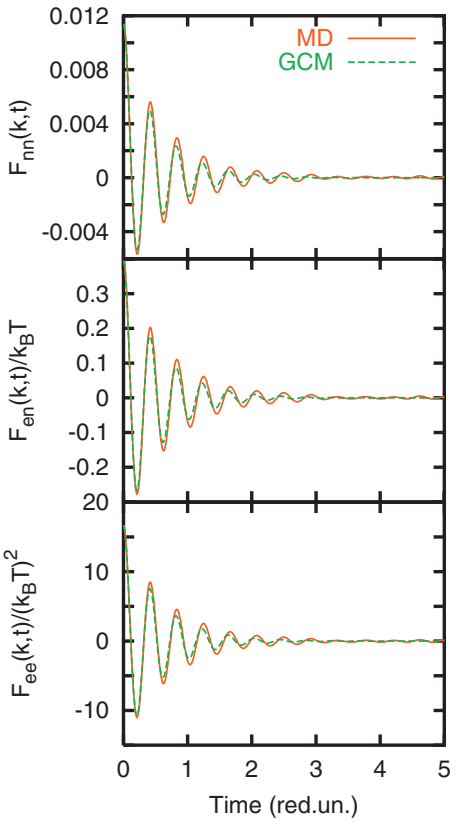

FIG. 2. Density-density, density-energy, and energy-energy time correlation functions at $k = 0.180$ Å^{-1}, derived from MD simulations (solid line), together with their GCM replicas (dashed lines). The high quality of GCM replicas is provided by exact reproduction of frequency sum rules up to the fourth frequency moment of dynamic structure factor. The time unit is $\tau = 5.1376$ ps.

Dynamic structure factors $S(k,\omega)$ are connected to the density-density time correlation functions via time Fourier transform. In Fig. 3 the dynamic structure factors, obtained numerically from MD-derived density-density time correlation functions (solid red lines), and those represented by the theoretical five-variable GCM approach (dashed green lines) are shown for three wave numbers. In general, good agreement is observed between the MD and theoretical curves, especially perfect reproduction of $S(k,\omega)$ by the five-variable GCM approach is obtained at low and high wave numbers. For intermediate wave numbers the theory leads to side peaks a little bit higher and narrower than those yielded by MD simulations, although they are located at the correct frequency of collective excitation. Besides the central peak is reproduced very nicely. In all cases the theoretical $S(k,\omega)$ have exactly the same frequency moments up to the fourth order as the MD-derived dynamic structure factors.

Having dynamic structure factors we can estimate the Landau–Placzek ratio, which in case of pure fluids is a measure of contributions from thermal processes (central peak of dynamic structure factor) and sound propagation (Brillouin peaks) to the long-wavelength collective dynamics. The ratio of integral intensities of central and side peaks of calculated

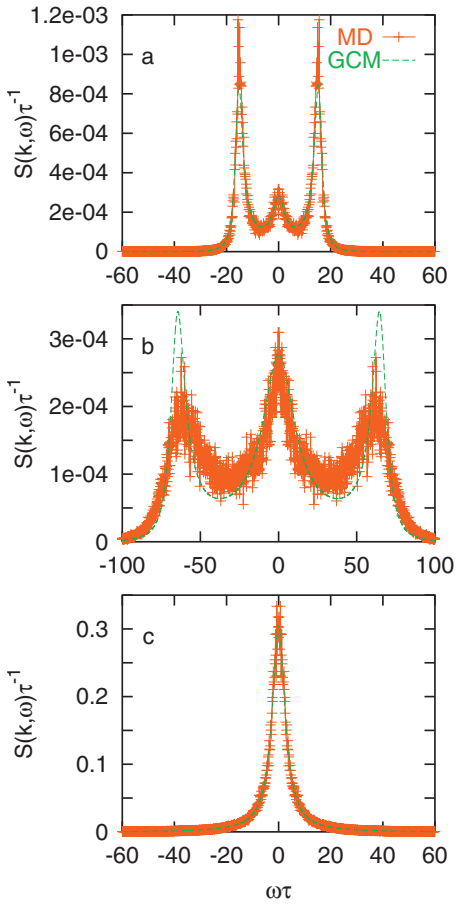

FIG. 3. Dynamic structure factors, obtained by time Fourier transformation of MD-derived time correlation functions (red solid lines) and corresponding GCM replicas (green dashed lines) for three wave numbers: $k=0.180$ Å^{-1} (a), 0.880 Å^{-1} (b), and 2.215 Å^{-1} (c). The time unit is the same as in Fig. 2.

$S(k,\omega)$ for the smallest wave number is ~0.17, that is in good agreement with the right hand side of relation,

$$\frac{I_{\text{central}}}{2I_{\text{side}}} = (\gamma - 1), \tag{4}$$

taking into account our calculated value of the ratio of specific heats γ. This is an evidence that the calculated dynamic properties are in good agreement with thermodynamics. We have to mention here, that for the case of many-component fluids the Landau–Placzek ratio has a more complicated form than Eq. (4). Recently we have shown on example of a molten binary alloy Li_4Tl (Ref. 16) how the Landau–Placzek ratio for binary systems takes into account concentration fluctuations.

C. Spectrum of collective excitations

1. Longitudinal modes

The pairs of complex-conjugated eigenvalues,

$$z_\alpha(k) = \sigma_\alpha(k) \pm i\omega_\alpha(k),$$

correspond to two collective excitations propagating in opposite directions with damping $\sigma_\alpha(k)$ and dispersion $\omega_\alpha(k)$. Dispersion and damping of the generalized sound excitations obtained from the analysis of the MD data within the five-variable dynamic model $\mathbf{A}^{(5)}(k,t)$ are shown in Fig. 4. In the long-wavelength range the $\omega_{\text{sound}}(k)$ displays a small "positive dispersion," which is usually treated as a consequence of coupling of the propagating longitudinal acoustic modes with nonhydrodynamic process of structural relaxation.[17] A straight dashed line corresponds to hydrodynamic sound dispersion with the adiabatic speed of sound $c_s=1648$ ms^{-1}. This value was obtained from the smooth extrapolation of our estimated k-dependence of $\sqrt{\gamma(k)/S(k)}$ to the limit $k\to 0$. The obtained value of adiabatic speed of sound is in good agreement with the experimental value of $c_{\text{exp}}=1663$ ms^{-1}.[18] The dispersion of the generalized sound excitations has a minimum at the position of the first peak of the static structure factor $S(k)$ that corresponds to their strong scattering (and damping) on the pseudo-Brillouin zone boundary.

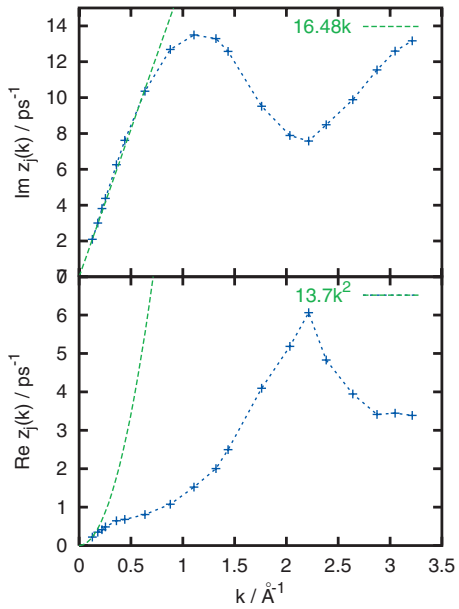

FIG. 4. Dispersion (top frame) and damping (bottom frame) of the generalized sound excitations. Dashed lines correspond to the observed hydrodynamic asymptotes with adiabatic sound velocity $c_s=1648$ ms^{-1} and damping coefficient $\Gamma=1.37\times10^{-7}$ m^2 s^{-1}.

The wave number dependence of the damping of the generalized sound excitations is shown in the bottom frame of Fig. 4. The corresponding hydrodynamic asymptote should be $\sigma(k)=\Gamma k^2$ with Γ being the sound damping coefficient. From the lowest k-points we were able to estimate the value of $\Gamma=1.37\times10^{-7}$ m^2/s. On the whole, $\sigma(k)$ shows a crossover from a quadratic dependence with k in the hydrodynamic region to an almost linear one in the interval 0.5 Å^{-1}–1.2 Å^{-1}. Similar features in the wave number dependence of damping of generalized acoustic excitations were observed previously for liquid Pb.[8] Besides, the sound damping reaches its maximum at the location of the main maximum of static structure factor ($k\sim2.2$ Å^{-1}).

Since Tl is a trivalent liquid metal it is interesting to compare the obtained results for long-wavelength longitudinal collective modes with the Bohm–Staver theory of collective excitations in metallic systems.[19,20] According to the

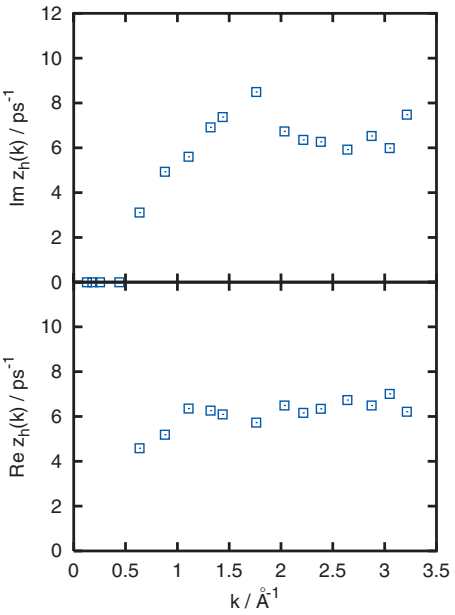

FIG. 5. Dispersion (top frame) and damping (bottom frame) of nonhydrodynamic heat waves in liquid Tl. For $k<0.62$ Å^{-1} the heat waves cannot propagate in this liquid.

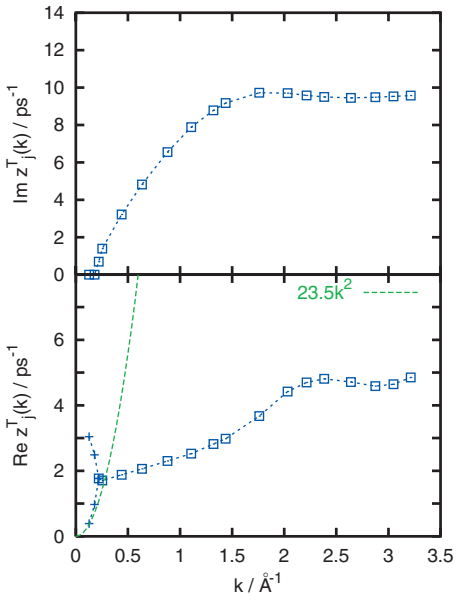

FIG. 6. Dispersion (top frame) and damping (bottom frame) of generalized shear waves (open boxes). A propagation gap appears below $k\approx0.22$ Å^{-1}. The complex pair of eigenvalues moves to a pair of purely real ones (plus symbols). The dotted line corresponds to the expected hydrodynamic asymptote of the lowest transverse relaxation process.

Bohm–Staver model the long-wavelength dispersion of acoustic excitations in metallic systems is expressed by a simple expression,

$$\omega_{\mathrm{BS}}^2(k)=\frac{1}{\epsilon(k)}\Omega_p^2,$$

where Ω_p is the ion plasma frequency and $\epsilon(k)$ is the static dielectric function of homogeneous electron gas that diverges in the long-wavelength limit as k^{-2}. Taking the $\epsilon(k)$ in the standard random phase approximation we have obtained for the speed of long-wavelength acoustic Bohm–Staver excitations in liquid Tl a value $c_{\mathrm{BS}}=2716.3$ m/s, that is more than 60% higher, that the experimental adiabatic speed of sound. This value supports an original assumption by Bohm and Staver,[19] that the non-Coulombic part of the interionic potential, which was ignored in the original Bohm–Staver model, is appreciable for polyvalent metals. We have to mention here recent attempts to improve the Bohm–Staver model by introducing low-k corrections to plasma dispersion and an account for finite mean square ionic radii.[21,22] These corrections work very nicely for alkali metals, however for dense metallic systems such as Al or Ga (with small GellMann–Bruckner parameters r_s of 2.191 and 2.426 Bohr radius, respectively) they must have yielded negative corrections to the Bohm–Staver dispersion.[22] It seems that the liquid Tl with $r_s=2.532$ a.u. is another polyvalent liquid metal in this row, for which the mentioned corrections should be negative.

A common feature of liquid metals studied before by the GCM approach[7–9] was the existence of another branch of propagating modes, which corresponded to nonhydrodynamic heat waves. The branch of nonhydrodynamic propagating collective modes appears in liquid Tl for wave numbers $k>0.62$ Å^{-1} (Fig. 5). This low-frequency branch corresponds to heat density propagating on distances not larger than 10–15 Å. On macroscopic scales the only mechanism of heat transfer is a relaxation process connected with thermal conductivity. To some extent the behavior of heat waves is similar to the dispersion of shear waves in liquids, and this analogy was known for years in continuum mechanics.[23] However, there are no studies of heat waves in MD simulations, except within the GCM approach.[8] Namely, the GCM approach can predict the width of the propagating gap for heat waves in long-wavelength region.[8] Inside the propagation gap, for $k<0.62$ Å^{-1} in liquid Tl, the heat transfer is only via hydrodynamic thermal relaxation. One can see in Fig. 5 that the damping of heat waves is larger than for sound excitations, that implies they contribute smaller to the density-density time correlation functions.

2. Transverse modes

Transverse dynamics of pure fluids can be analyzed within the two-variables dynamic model $\mathbf{A}^{(2T)}$ Eq. (2), where the only extended dynamic variable is the first time derivative of the hydrodynamic transverse momentum density. The corresponding transverse eigenvalues are shown in Fig. 6. In the top frame one can see that there exists a propagation gap for the long-wavelength transverse collective excitations in complete agreement with the hydrodynamic theory. From our analysis, the width of the propagation gap of shear waves is $k_s\approx0.22$ Å^{-1} for liquid Tl at the melting point. Beyond this gap the dispersion of shear modes (imaginary parts of transverse complex eigenvalues) shows a steep increase followed by an almost flat part for $k>1.5$ Å^{-1}. The damping of shear waves (real parts of complex eigenvalues) increases almost linearly from k_s up to about 2 Å^{-1} where the curve reaches a plateau.

For wave numbers $k<k_s$, one obtains two purely real eigenvalues instead of the pair of complex-conjugated ones.

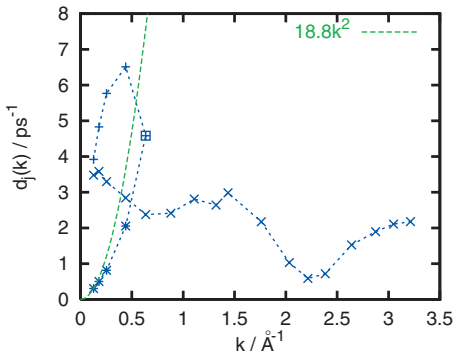

FIG. 7. Wave number-dependent relaxation processes in liquid Tl. The lowest real eigenvalue $d_1(k)$ in long-wavelength limit (stars) has a correct hydrodynamic asymptote (dashed line) and corresponds to relaxation processes connected with thermal diffusivity (dotted line). Estimated value of thermal diffusion coefficient is $D_T=1.88\times10^{-7}$ m^2 s^{-1}. The eigenvalue $d_2(k)$ (crosses) corresponds to structural relaxations and for $k>0.5$ Å^{-1}; it is the slowest relaxation process in the melt. Above 0.62 Å^{-1}, both $d_1(k)$ (stars) and $d_3(k)$ (plus) merge into a single propagating branch (squares) corresponding to heat waves, which is shown in Fig. 5.

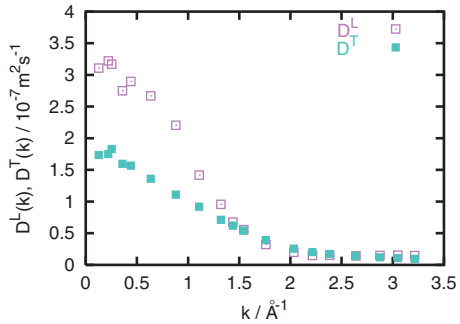

FIG. 8. Generalized wave number-dependent kinematic viscosity $D^L(k)$ (open boxes) and shear viscosity $D^T(k)=\eta_s(k)/\rho$ (filled boxes).

They are shown by line-connected "plus" symbols in Fig. 6. The lowest real eigenvalue in the long-wavelength limit must behave as

$$d_1^T(k) = D^T k^2,$$

where $D^T(k)=\eta_s(k)/\rho$ with $\eta_s(k)$ being the shear viscosity and ρ, mass density. The dashed line in the bottom frame of Fig. 6 corresponds to this hydrodynamic asymptote and allows to estimate the value of the shear viscosity at 0.026 P.[10] The real eigenvalue with the shorter lifetime, $d_2^T(k)$, corresponds to a kinetic transverse relaxation process. Analytical results for the transverse real modes[9] make evidence, that the long-wavelength limit of the $d_2^T(k)$ is defined by the shear modulus.

D. Wave number-dependent relaxation processes

One can distinguish between two kinds of relaxation processes: hydrodynamic ones with corresponding relaxation times proportional to k^{-2} and nonhydrodynamic (kinetic) ones with finite relaxation times in the hydrodynamic limit. For longitudinal dynamics in pure liquids, the only hydrodynamic relaxation process in the region of small wave numbers is the one connected with thermal diffusivity. This relaxation process makes the leading contribution to the central peak of dynamic structure factor $S(k,\omega)$ in long-wavelength region. In Fig. 7 we show the purely real eigenvalues $d_j(k), j=1,\ldots3$ of the generalized hydrodynamic matrix and corresponding to wave number-dependent relaxation processes. In the long-wavelength range the lowest real eigenvalue $d_1(k)$ behaves almost proportionally to k^2. This allows to ascribe it to the hydrodynamic mode and to estimate the value of the thermal diffusivity at $D_T=1.88\times10^{-7}$ m^2 s^{-1}. The other two real eigenvalues tend to nonzero values in the long-wavelength limit that means finite relaxation times on macroscopic distances (in comparison with the k^{-2} asymptote of hydrodynamic processes). According to analytical solutions of the dynamic model $\mathbf{A}^{(5)}(k,t)$ (Ref. 13) the relaxation mode $d_2(k)$ shown by crosses in Fig. 7 tends to a long-wavelength limit,

$$d_2(0) = \frac{c_\infty^2 - c_s^2}{D_L},$$

that is known as the strength of the structural relaxation.[17,24] In this former expression, c_∞ denotes the high-frequency speed of sound and D_L, the kinematic viscosity. Hence, the relaxation process $d_2(k)$ is the wave number-dependent structural relaxation. One of its most interesting features is a crossover with the hydrodynamic relaxation mode $d_1(k)$ at $k\approx0.5$ Å^{-1}. For larger wave numbers $d_2(k)$ becomes the slowest relaxation process in the system on short length scales, while on macroscopic ones the slowest relaxation process is the one connected with thermal diffusion $d_1(k)$. This explains why viscoelastic theories are very successful in describing the collective dynamics on intermediate and short length scales.

The third real eigenvalue $d_3(k)$ shown by plus symbols in Fig. 7 corresponds to a fast kinetic thermal relaxation process. Both thermal processes $d_1(k)$ and $d_3(k)$ merge for $k\geq0.62$ Å^{-1}. In this region the kinetic heat waves emerge instead of the two thermal relaxation processes and bring an additional mechanism of heat transport on microscopic distances, while heat waves cannot exist in liquids on macroscopic distances in complete agreement with hydrodynamics.

E. Generalized transport coefficients

The generalized wave number- and frequency-dependent transport coefficients can be calculated from the matrix of lowest order (hydrodynamic) memory functions $\tilde{\mathbf{M}}(k,\omega)$ [6,25] as follows:

$$\tilde{\mathbf{M}}(k,\omega) = k^2 V k_B T \tilde{\mathbf{L}}(k,\omega)\mathbf{F}(k,t=0), \quad (5)$$

where $\tilde{\mathbf{L}}(k,\omega)$ is the 3×3 matrix of generalized wave number- and frequency-dependent transport coefficients, V is the volume of the system, and T is the temperature. In such a way we obtained the generalized static kinematic viscosity $D^L(k,\omega=0)$ and thermal conductivity $\lambda(k,\omega=0)$. In the case of transverse dynamics we calculated similarly the wave number-dependent shear viscosity $\eta_s(k,\omega=0)=\rho D^T(k,\omega=0)$, where ρ is the mass density of the system.

In Fig. 8 the wave number dependences of $D^L(k)$ and

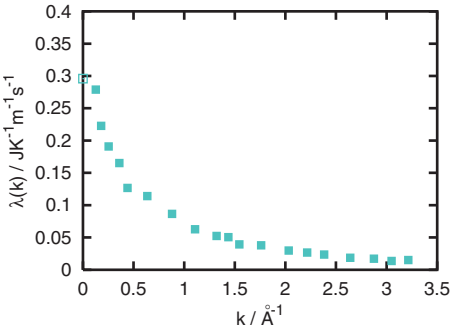

FIG. 9. Generalized wave number-dependent thermal conductivity $\lambda(k)$. The value $\lambda(k=0)$ shown by open box was obtained from thermal diffusivity and specific heat at constant pressure.

$D^T(k)$ are shown. The kinematic viscosity can be represented as a sum of contributions from shear (η_s) and bulk viscosities (η_v),

$$D^L(k) = \frac{4}{3}D^T(k) + \frac{\eta_v(k)}{\rho} = \frac{4}{3}\frac{\eta_s(k)}{\rho} + \frac{\eta_v(k)}{\rho}. \quad (6)$$

It is observed that the kinematic viscosity tends to a macroscopic value $D^L \approx 3\times 10^{-7}$ m^2/s, while the shear viscosity corresponds to the value of $D^T \approx 2.35\times 10^{-7}$ m^2/s. Interestingly, according to Eq. (6) and Fig. 8, the contribution from bulk viscosity to $D_L(k)$ is decreasing with wave number and the generalized bulk viscosity $\eta_v(k)$ even becomes negative in the region of $k>1.7$ Å^{-1}. This change of sign happens in the range of wave numbers, where the generalized linear thermal expansion coefficient becomes also negative (Fig. 1). However, the generalized bulk viscosity becomes again positive for $k>2.5$ Å^{-1}. One has to mention that a similar feature of the wave number dependence, namely, a negative range of generalized bulk viscosity was previously reported for Lennard-Jones fluids.[25]

The generalized thermal conductivity is shown in Fig. 9. In general it is a monotonically decaying function of k, which tends to the macroscopic value of the ionic part of the thermal conductivity in the long-wavelength limit. In the case of liquid metals, we stress that another contribution to the thermal conductivity comes from the electronic excitations (Fermi liquid), which is impossible to obtain in the frame of classical MD. The ionic part of the thermal conductivity obtained in this study is in complete agreement with the value reported in the previous section about thermal relaxation processes and obtained from thermodynamic quantities such as specific heat at constant volume and ratio of specific heats (see Fig. 1). In Fig. 9, we show by open box at $k=0$ the value of $\lambda=0.296$ J/(s m K) obtained from the reported above quantities using the relation

$$\lambda = nC_pD_T,$$

where n is number density and D_T, the thermal diffusivity. The agreement between both approaches for the estimation of λ is very good.

IV. CONCLUSION

We have studied the collective modes and generalized transport coefficients in the polyvalent liquid metal Tl at its melting point. The parameter-free GCM approach was applied to estimate the spectrum of dynamic eigenmodes including collective excitations and nonpropagating wave number-dependent relaxation processes. The pair potentials derived from Fiolhais pseudopotential permit to simulate correctly the heat fluctuations in the liquid polyvalent metal and obtain the ratio of specific heats close to its experimental value. The obtained eigenmodes and eigenvectors permitted to reproduce very well the MD-derived time correlation functions without any fitting, demonstrating the accuracy of the dynamic model chosen for this theoretical study.

The calculated value of the adiabatic speed of sound is in very good agreement with experimental data. We also predict a small positive deviation of long-wavelength acoustic excitations from a linear dispersion law. It was shown that in the region $k>0.62$ Å^{-1} there exists another branch of collective propagating modes that correspond to nonhydrodynamic heat waves. In complete agreement with hydrodynamics of liquids, they cannot exist in the long-wavelength range, supporting an analogy with shear waves known from continuum mechanics.[23]

Wave number-dependent thermodynamic quantities and transport coefficients were estimated for liquid Tl. We obtained perfect agreement with the macroscopic value for the calculated generalized ratio of specific heats. The wave number dependence of generalized linear thermal expansion coefficient reveals negative values of $\alpha_T(k)$ in the region 2.1 Å$^{-1}>k>1.6$ Å^{-1} that is similar to the observation for the case of liquid Pb close to its melting point[8] and can be a precursor of bonding correlations on nanoscale at the melting point. The generalized kinematic and shear viscosities show a standard monotonically decaying wave number dependence. For 2.5 Å$^{-1}>k>1.7$ Å^{-1}, our calculations suggest that the bulk viscosity of liquid Tl becomes negative, similar to the reported for Lennard-Jones fluids.[25] The region of wave numbers with negative bulk viscosity corresponds to the region with negative generalized linear thermal expansion coefficient.

ACKNOWLEDGMENTS

T.B. was supported by the Joint SFBRU-RFBR Program under Project No. Φ28.2/037.

[1] J.-P. Hansen and I. R. McDonald, *Theory of Simple Liquids* (Academic, London, 1986).
[2] T. Scopigno, G. Ruocco, and F. Sette, Rev. Mod. Phys. **77**, 881 (2005).
[3] J.-P. Boon and S. Yip, *Molecular Hydrodynamics* (McGraw-Hill, New York, 1980).
[4] C. Cohen, J. W. H. Sutherland, and J. M. Deutch, Phys. Chem. Liq. **2**, 213 (1971).
[5] T. Scopigno, U. Balucani, G. Ruocco, and F. Sette, J. Phys.: Condens. Matter **12**, 8009 (2000).
[6] I. M. Mryglod, Condens. Matter Phys. **1**, 753 (1998).
[7] T. Bryk and Y. Chushak, J. Phys.: Condens. Matter **9**, 3329 (1997).
[8] T. Bryk and I. Mryglod, Phys. Rev. E **63**, 051202 (2001).
[9] T. Bryk and I. Mryglod, J. Phys.: Condens. Matter **12**, 6063 (2000).
[10] A. F. Crawley, Trans. Metall. Soc. AIME **242**, 2309 (1968).
[11] E. B. El Mendoub, R. Albaki, I. Charpentier, J.-L. Bretonnet, J.-F. Wax, and N. Jakse, J. Non-Cryst. Solids **353**, 3475 (2007).
[12] Y. Waseda, *The Structure of Non-Crystalline Materials* (McGrawHill, New York, 1980).
[13] T. Bryk and I. Mryglod, Condens. Matter Phys. **7**, 471 (2004).

[14] I. M. de Schepper, E. G. D. Cohen, C. Bruin, J. C. van Rijs, W. Montfrooij, and L. A. de Graaf, Phys. Rev. A **38**, 271 (1988).
[15] I. M. Mryglod, I. P. Omelyan, and M. V. Tokarchuk, Mol. Phys. **84**, 235 (1995).
[16] T. Bryk and J.-F. Wax, Phys. Rev. B **80**, 184206 (2009).
[17] T. Bryk and I. Mryglod, Condens. Matter Phys. **11**, 139 (2008).
[18] Y. Tsuchiya and F. Kakinuma, J. Phys.: Condens. Matter **4**, 2117 (1992).
[19] D. Bohm and T. Staver, Phys. Rev. **84**, 836 (1951).
[20] D. Pines and P. Nozieres, *The Theory of Quantum Liquids* (Benjamin, New York, 1966).
[21] L. E. Bove, F. Formisano, F. Sacchetti, C. Petrillo, A. Ivanov, B. Dorner, and F. Barocchi, Phys. Rev. B **71**, 014207 (2005).
[22] L. E. Bove, C. Petrillo, and F. Sacchetti, Condens. Matter Phys. **11**, 119 (2008).
[23] D. D. Joseph and L. Preziosi, Rev. Mod. Phys. **61**, 41 (1989).
[24] C. Masciovecchio, F. Bencivenga, and A. Gessini, Condens. Matter Phys. **11**, 47 (2008).
[25] I. M. Mryglod and I. P. Omelyan, Mol. Phys. **92**, 913 (1997).